

## **Pool Boiling Heat Transfer in Annuli with Closed Bottom**

**Myeong-Gie Kang and Young-Hwan Han**

Andong National University  
388 Songchun-dong, Andong-city, Kyungbuk, 760-749, Korea  
mgkang@andong.ac.kr

(Received October 15, 2001)

### **Abstract**

Effects of gap sizes (3.9-44.3 mm) of vertical annuli on nucleate pool boiling heat transfer of water at atmospheric pressure have been obtained experimentally. Through the study, tubes of the closed bottom have been investigated and results are compared with those of a single unconfined tube. According to the results, the annular condition gives much increase in heat transfer coefficient at moderate heat fluxes. The increase is much enhanced as the gap size decreases. At the same tube wall superheat (about 3.1 K) the heat transfer coefficient for the least gap size (i.e., 3.9 mm) is more than three times greater than that of the unconfined tube. However, deterioration of heat transfer occurs at high heat flux for confined boiling.

**Key Words** : pool boiling, heat transfer, annuli condition, closed bottom, passive heat exchanger, gap size, tube

### **1. Introduction**

The mechanism of pool boiling heat transfer has been studied extensively in the past [1] since it is closely related with the thermal design of more efficient heat exchangers. Recently, it has been widely investigated in nuclear power plants for application to the design of new passive safety systems employed in the advanced light water reactors [2,3]. To determine the required heat transfer surface area as well as to evaluate the system performance during postulated accidents, overall heat transfer coefficients applicable for the passive heat exchangers are needed. Although

many workers have investigated effects of heater geometries on boiling heat transfer in the past two generations [4], knowledge on the confined spaces on pool boiling heat transfer is still very limited. However, crevice effects in flow boiling have been widely studied [5-7].

Studies on the crevices can be divided into two categories. One of them is about annuli [8-10] and the other one is about plates [11,12]. Some previous results about crevice effects on pool boiling heat transfer are listed in Table 1. In addition to the geometric condition, flow to the crevices can be limited, too. Some geometry has a closed bottom [8,11]. For the case, fluid should be

**Table 1. Previous Works About Crevice Effects on Pool Boiling Heat Transfer**

Author	Remarks
Yao and Chang (1983)	<ul style="list-style-type: none"> <li>- heater: stainless steel tube (<math>D=25.4\text{mm}</math>, <math>L=25.4</math> and <math>76.2\text{mm}</math>)</li> <li>- liquid: R-113, acetone, and water at 1 atm</li> <li>- geometry: vertical annuli with closed bottoms</li> <li>- gap sizes: 0.32, 0.80, and 2.58mm</li> <li>- main conclusions:               <ul style="list-style-type: none"> <li>• R-113; <math>h_b</math> increases when gap size decreases at low heat fluxes whereas it decreases at higher heat fluxes</li> <li>• water and acetone; <math>h_b</math> increases when gap size decreases to a certain value (at present, 0.80mm)</li> </ul> </li> </ul>
Hung and Yao (1985)	<ul style="list-style-type: none"> <li>- heater: stainless steel tube (<math>D=25.4\text{mm}</math>, <math>L=25.4\sim 76.2\text{mm}</math>)</li> <li>- liquid: R-113, acetone, and water at 1 atm</li> <li>- geometry: horizontal annuli</li> <li>- gap sizes: 0.32, 0.80, and 2.58mm</li> <li>- main conclusions:               <ul style="list-style-type: none"> <li>• R-113; <math>h_b</math> increases when gap size decreases at low heat fluxes whereas it decreases at higher heat fluxes</li> <li>• water and acetone; <math>h_b</math> increases when gap size decreases to a certain value (at present, 0.80mm)</li> <li>• very large oscillation of temperatures is observed when the gap size is 0.32mm</li> <li>• the CHF decreases with decreasing gap size</li> </ul> </li> </ul>
Fujita et al. (1988)	<ul style="list-style-type: none"> <li>- heater: copper plate (<math>30\times 30</math> and <math>30\times 120\text{mm}</math> in width <math>\times</math> length)</li> <li>- liquid: water at 1 atm</li> <li>- geometry:               <ul style="list-style-type: none"> <li>• vertical and inclined spaces between rectangular surfaces</li> <li>• periphery; open, closed sides, closed sides and bottom</li> </ul> </li> <li>- gap sizes: 0.15, 0.60, 2.0 and 5.0mm</li> <li>- main conclusions:               <ul style="list-style-type: none"> <li>• <math>h_b</math> increases up to a certain maximum value (at present, 0.60mm) with decrease of the gap size at moderate heat fluxes</li> <li>• periphery closure gives increase in <math>h_b</math> to a certain maximum value with decrease of the gap size at moderate heat fluxes</li> <li>• further increasing heat flux, <math>h_b</math> for the closed periphery cases converges to the case of the unconfined tube</li> </ul> </li> </ul>
Bonjour and Lallemand (1998)	<ul style="list-style-type: none"> <li>- heater: copper plate (<math>60\times 120\text{mm}</math> in width <math>\times</math> length)</li> <li>- liquid: R-113 at 1 atm</li> <li>- geometry:               <ul style="list-style-type: none"> <li>• vertical and inclined space between rectangular surfaces</li> <li>• periphery; sides and bottom are left open</li> </ul> </li> <li>- gap sizes: 0.3, 0.50, 1.0 and 2.0mm</li> <li>- main conclusions:               <ul style="list-style-type: none"> <li>• <math>h_b</math> increases as the gap size decreases at low heat fluxes</li> <li>• <math>h_b</math> deterioration and a noticeable decrease in CHF occur at high heat fluxes</li> </ul> </li> </ul>
Kang (2001)	<ul style="list-style-type: none"> <li>- heater: stainless steel tube (<math>D=25.4\text{mm}</math>, <math>L=570\text{mm}</math>)</li> <li>- liquid: water at 1 atm</li> <li>- geometry: vertical annuli with open or closed bottoms</li> <li>- gap sizes: 3.9 and 15mm</li> <li>- main conclusions:               <ul style="list-style-type: none"> <li>• effects of annular geometry is much enhanced with the bottom blockage</li> <li>• <math>h_b</math> deterioration is observed as the heat flux is more than <math>70\text{ kW/m}^2</math> when the gap size is 3.9 mm for the closed bottom condition</li> </ul> </li> </ul>

supplied and be discharged through the open side only.

It is well known from the literature that the confined boiling is an effective technique to enhance heat transfer. It can result in heat transfer improvements up to 300%-800% at low heat fluxes, as compared with unconfined boiling [8,11]. However, deterioration of heat transfer appears at high heat fluxes for confined boiling [11,12]. The effect of gap sizes on pool boiling is fluid dependent and this can change the general trend mentioned above [8,9]. The boiling heat transfer coefficient ( $h_b$ ) usually increases when gap size decreases at low heat fluxes whereas it decreases at higher heat fluxes. However, increases when gap size decreases to a certain value [8,9,12]. Further decrease in gap size results in sudden decrease in  $h_b$ . Summarizing the previous works about crevice effects on pool boiling heat transfer it can be concluded that the amount of  $h_b$  is highly dependent on the geometry and confinement condition.

Through the literature survey, it can be said that studies about annuli with longer heating surface are rarely found. Although Kang [10] recently published some results for two gap sizes (i.e., 3.9 and 15.0 mm) of the annuli with open or closed bottoms, it is still necessary to add some more data to elucidate the heat transfer mechanisms in annuli. Moreover, one of the most important factors in heat exchangers design for application to the advanced light water reactors is to find a way to increase heat transfer coefficients [1] and those heat exchangers have usually very long heating tubes. Therefore, to investigate the potential areas for improvement of the thermal design of the heat exchangers and to add some data on the previous work by others, nucleate pool boiling heat transfer in annuli and tubes of water has been investigated at atmospheric pressure.

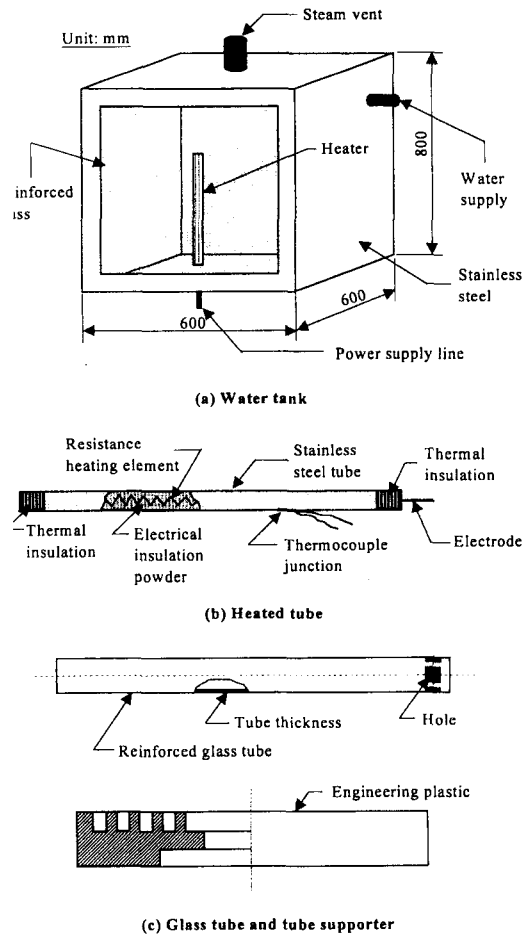


**Fig. 1. Schematic Diagram of the Experimental Apparatus**

## 2. Experiments

A schematic view of the present experimental apparatus and test sections is shown in Fig. 1. The water storage tank is made of stainless steel and has a rectangular cross section (600 × 600 mm) and a height of 800 mm. This tank has a glass view port (500 × 700 mm) which permits viewing of the tubes and photographing. To reduce heat loss to the environment, every wall, except the front side, of the tank were insulated by glass wool

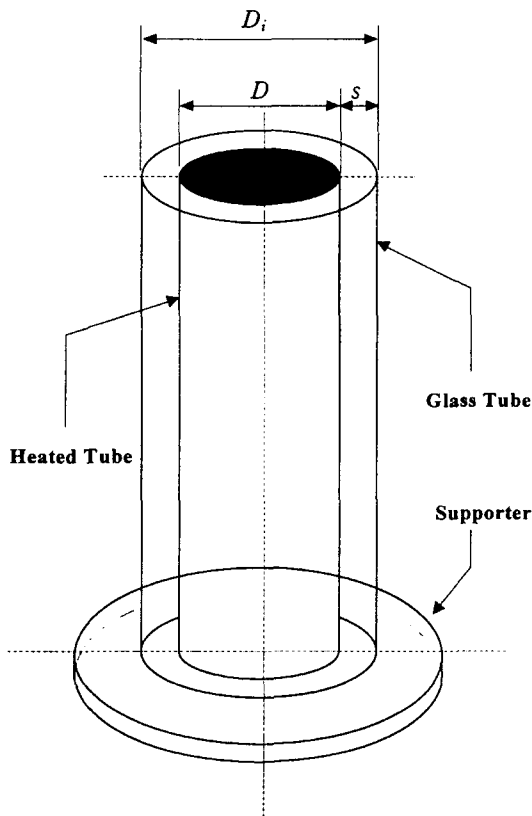


**Fig. 2. Schematic of the Fabricated Test Section**

of 30 mm in thickness. The heat exchange tube is made of stainless steel ( $L=500$  mm and  $D=25.4$  mm). To get uniform and smooth surface the tube surface was manufactured through buffing process by a buffing machine.

The surface temperatures of the tube were measured with five T-type sheathed thermocouples (diameter is 1.6 mm) outside the surface of the tube. The thermocouple tip (about 10 mm) has been bent at a 90 degree angle and brazed the bent tip on the tube wall. The locations of the thermocouples are 50, 150, 250, 350, and 450 mm from the bottom of the heated tube length. The water temperatures were measured with seven sheathed T-type thermocouples placed at the tank wall vertically from the tank bottom

with equal space (i.e., 100 mm). All thermocouples were calibrated at the boiling point (i.e., 100 °C).

For the tests, the heat exchange tube is placed at the tank bottom and a tube supporter is used to fix the glass tubes (see Fig. 2). To make annular conditions, five glass tubes having different inside diameters ( $D$ ) were used. Therefore, gap sizes ( $s$ ) of the annuli are between 3.9 and 44.3 mm. The side without holes is placed at the tank bottom for the closed bottom tests. In addition, all periphery of the bottom side of the glass tube was sealed with silicon. A fixture made of three slim wires of 1.6 mm in diameter was inserted into the upper side of the gap to keep the space between the heating tube and the glass tube.

After the water storage tank is filled with water until the initial water level is reached at 730 mm, the water is then heated using three pre-heaters at constant electrical power (i.e., 5 kW/heater). Through the heating process, temperatures of the water were measured. When the water temperature is reached at a saturation value (i.e., 100 °C since all the tests are run at atmospheric pressure condition), the water is then boiled for 30 minutes at saturation temperature to remove the dissolved air. Thereafter, the temperatures of the water and tube surfaces are measured when they are at steady state while controlling the heat flux on the tube surface with input power. The uncertainty in the heat flux and the measured temperature is estimated to be  $\pm 1.0$  % and  $\pm 0.5$  K, respectively. The uncertainty for the temperature includes errors from thermocouple brazing, compensation, multiplexer itself, and thermocouple sensing. The uncertainty of the calculated heat transfer coefficients (i.e.,  $h_b=q''/\Delta T_{sat}$ ) depends on the superheat and heat flux. For example, it is  $\pm 12.5$  % as  $q''=80$  kW/m<sup>2</sup> and  $\Delta T=5$ K.

The heat flux from the electrically heated tube surface is calculated from the measured values of

the power input as follows:

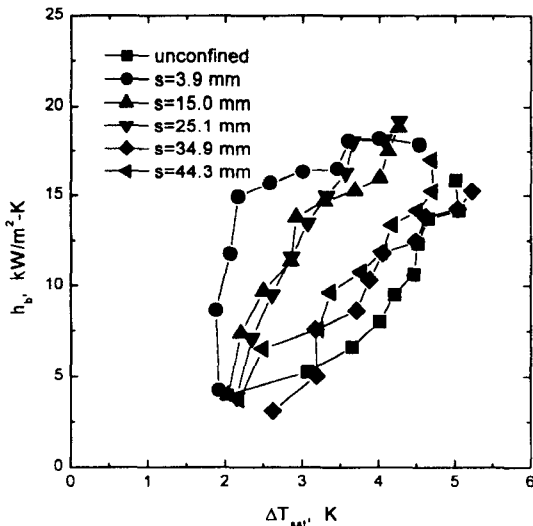
$$q'' = \frac{q}{A} = \frac{VI}{\pi DL} = h_b(T_w - T_{sat}) = h_b \Delta T_{sat} \quad (1)$$

where  $V$  and  $I$  are the supplied voltage (in volt) and current (in ampere), and  $L$  and  $T_w$  are the outside diameter and the length of the heated tube, respectively.  $T_w$  and  $T_{sat}$  represent the measured temperatures of the tube surface and the saturated water, respectively. The tube surface temperature  $T_w$  used in Eq. (1), on the other hand, is the arithmetic average value of the temperatures measured by five thermocouples brazed on the tube surface.

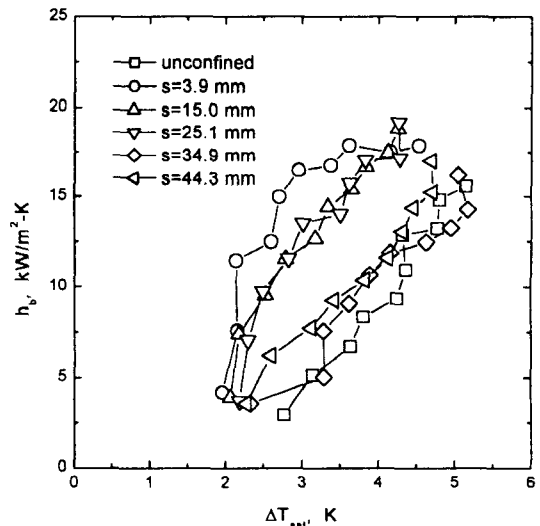
### 3. Results and Discussion

The experimental results of  $h_b$  versus  $\Delta T_{sat}$  for the annuli with open and closed bottoms are shown in Fig 3. The annular condition results in much increase in heat transfer coefficient. The increase is much enhanced as the gap size

decreases at lower tube wall superheats (i.e.,  $\Delta T_{sat} < 3.5$  K). At the same tube wall superheat (about 3.1 K) the heat flux of the least gap size (i.e.,  $s=3.9$  mm) is more than three times greater than that of the unconfined tube as  $\Delta T_{sat}$  increases (see Fig. 3(a)). For the case of larger gap sizes (i.e.,  $s=34.9$  and  $44.3$  mm) curves of  $h_b$  versus  $\Delta T_{sat}$  are somewhat similar to those of the unconfined tube case. However, as the gap size between the heating tube and the glass tube gets smaller the curve for  $h_b$  versus  $\Delta T_{sat}$  becomes to be linear (see curves of  $s=15.0$  and  $34.9$  mm). And, finally, the curve for  $s=3.9$  mm shows a kind of reverse slope comparing to that of the unconfined case. One of the possible causes for the phenomenon is liquid agitation and bubble coalescence. As the space gets narrower the intensity of liquid agitation due to bubbles gets stronger at first stage. This liquid agitation results in heat transfer increase. In other word, since much more liquid should be agitated for the case of the unconfined tube than the confined tube cases, heat transfer for the



(a)  $q''$  increase



(b)  $q''$  decrease

Fig. 3. Heat Transfer Coefficient Versus Tube Wall Superheat

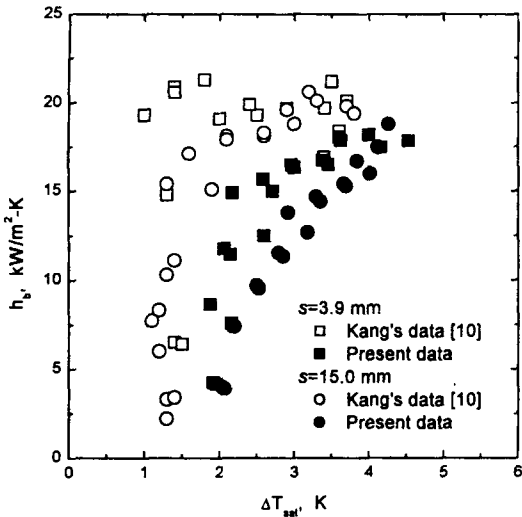
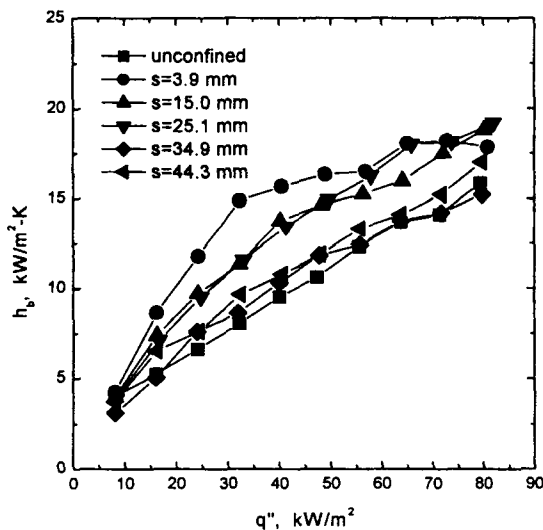


Fig. 4. Comparison of the Present Data with Kang's Data[10]

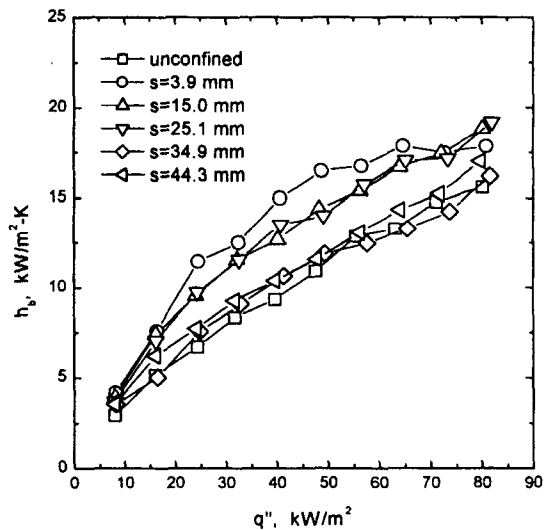
unconfined tube is accordingly less than the confined cases. For the confined tubes, because the departed bubbles not go far from the heating surface, these bubbles agitate relevant liquid very

much and increase heat transfer rate. Once the bottom side is closed, very strong liquid agitation and, accordingly, sudden increase in the heat transfer coefficient is observed. For the case of the closed bottom, more complicated bubble and liquid mixing is observed than the case of the open bottom since liquid should enter the upper side as the bubbles get out from it [10]. Therefore, bubbles fluctuating upward and downward according to the liquid entering and generate active liquid agitation. However, as the gap size is very small ( $s=3.9$  mm for the case) and  $\Delta T_{sat}$  increases more than 2.1 K, the liquid supply to the heating surface is not sufficient due to the interruption by bubble slugs. Therefore, an abrupt bubble slug formation is observed around the tube surface even at a low tube wall superheat. These bubbles result in deterioration in heat transfer coefficient.

To compare present experimental data with Kang's data [10] results of  $h_b$  versus  $\Delta T_{sat}$  are plotted as shown in Fig. 4. The general tendencies



(a)  $q''$  increase



(b)  $q''$  decrease

Fig. 5. Heat Transfer Coefficient Versus Heat Flux

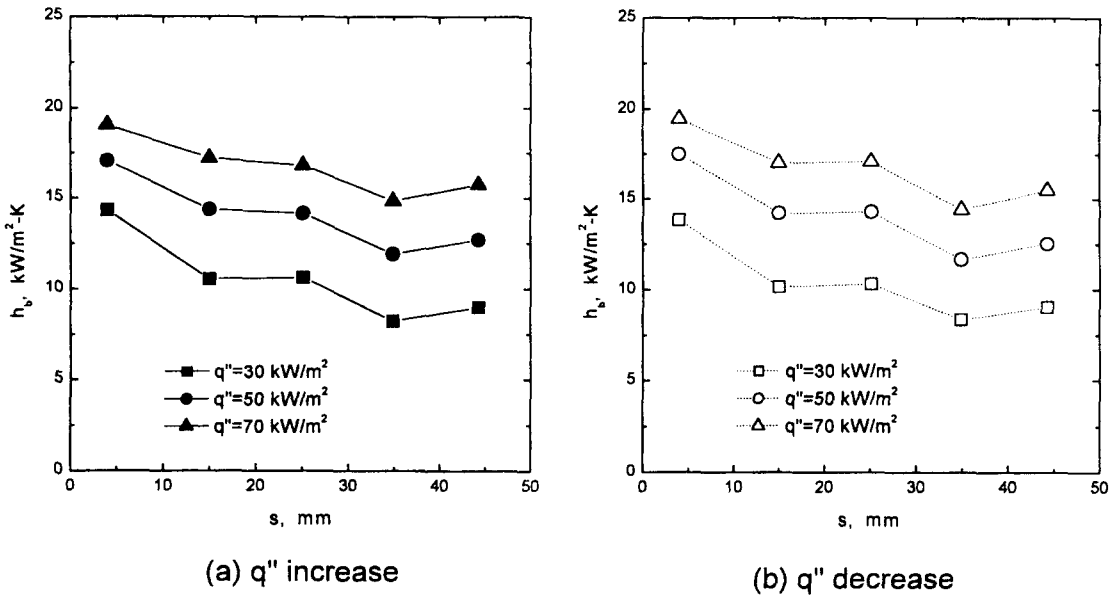


Fig. 6. Changes in Heat Transfer Coefficients due to Gap Size Change

of the two cases are very similar. However, values of  $h_b$  for the fixed  $\Delta T_{sat}$  are different from each other. One of the major causes for the difference in heat transfer coefficients for the same gaps size and tube wall superheat is the difference in tube surface condition. The tubes used in Kang's experiment were processed through a cold drawing whereas the present tubes were manufactured through a buffing process. A visual observation of two tube surfaces say that the present one is much smoother than those one used in Kang's test. If a tube has rougher surface more bubbles generated earlier than the smoother tube. This bubble results in very rapid increase in  $h_b$  even at a small  $\Delta T_{sat}$ . Therefore, bigger heat transfer coefficients are expected for the rougher tube case. However, the increase in bubble generation also results in earlier bubble slug formation around the upper region of the tube. Therefore, earlier deterioration in heat transfer coefficient is expected for the rougher tube case than the smoother tube as shown in Fig. 4. The

difference in tube length also can be a possible cause for the difference.

Changes in heat transfer coefficient as heat flux increases are shown in Fig 5. As shown in the figure the decrease in gap size enhances heat transfer coefficients. However, a deterioration of heat transfer occurs at high heat flux for confined boiling. At  $q'' = 30 \text{ kW/m}^2$  the slope of  $h_b$  versus curve starts to reduce (see the results for  $s = 3.9 \text{ mm}$ ). The smaller gap size, the earlier onset of  $h_b$  deterioration occurs.

Figure 6 shows results of the calculated heat transfer coefficients versus the gap size for various heat fluxes. All curves are results of curve fitting as third order polynomials for the experimental versus data. Numeric values of the parameters for the polynomial equations are listed in Table 2. As shown in the figure, there are no plausible hysteresis due to heat flux increase and decrease as Kang [13] proposed for the case of water and the smooth stainless steel tube [13]. As the gap size is changing from 34.9 mm to 3.9 mm and

**Table 2. Results of the Curve Fitting for  $h_b$  Versus  $q''$  Data (equation :  $h_b = A+B_1 (q'')^2+B_2 (q'')^3$ )**

s(mm)	A	Heat flux increase $B_1$	$B_2$	$B_3$
3.9	-1.57641	0.80948	-0.01187	6.03647E-5
15.0	-0.35818	0.59312	-0.00826	4.79147E-5
25.1	0.60138	0.43413	-0.00338	1.03921E-5
34.9	0.41617	0.34499	-0.00283	1.03864E-5
44.3	1.09086	0.37309	-0.00438	2.73789E-5
		Heat flux decrease		
3.9	-0.35060	0.59864	-0.00636	2.13693E-5
15.0	0.28617	0.51741	-0.00642	3.55927E-5
25.1	-0.43648	0.57118	-0.00748	4.16207E-5
34.9	0.20437	0.39953	-0.00489	2.87539E-5
44.3	0.92742	0.37606	-0.00457	2.98608E-5

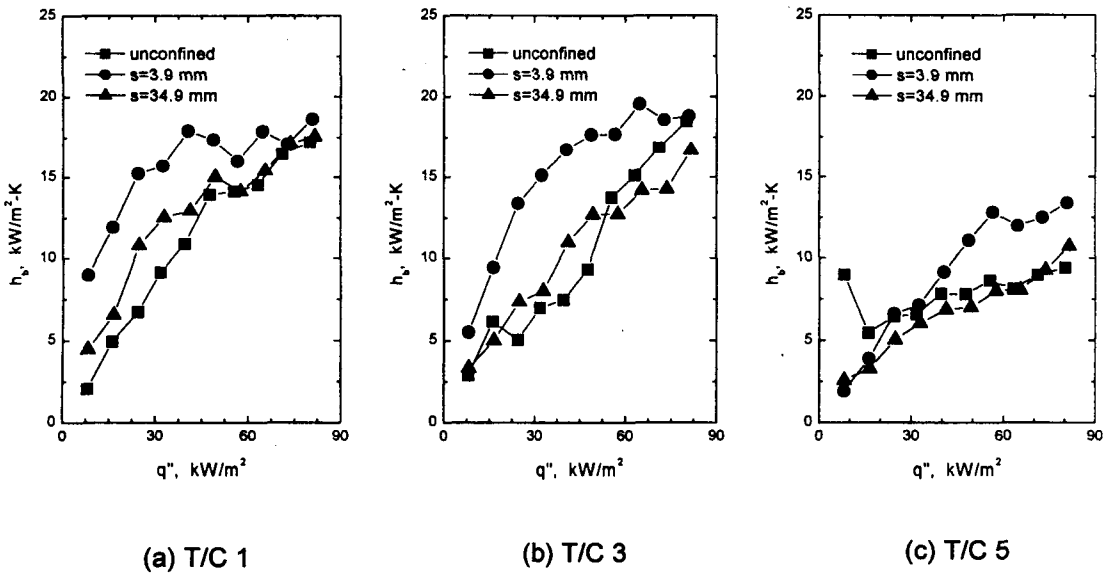


**Fig. 7. Changes in Heat Transfer Coefficients due to Thermocouple Location ( $T/C1=450\text{mm}$ ,  $T/C3=250\text{mm}$ , and  $T/C5=50\text{mm}$  from the heated tube bottom)**

$=70 \text{ kW/m}^2$ , increases in  $h_b$  is about 26%.

To get more clear heat transfer mechanism local heat transfer coefficients through the tube length are calculated using the measured heat fluxes and the thermocouple readings. Results of  $h_b$  versus  $q''$

are shown in Fig 7. Since increase in heat flux also results in increase in active nucleation site density,  $h_b$  increases linearly as  $q''$  increases at low heat fluxes. However, since liquid in and bubbles out is through the upper side only, bubbles escape is



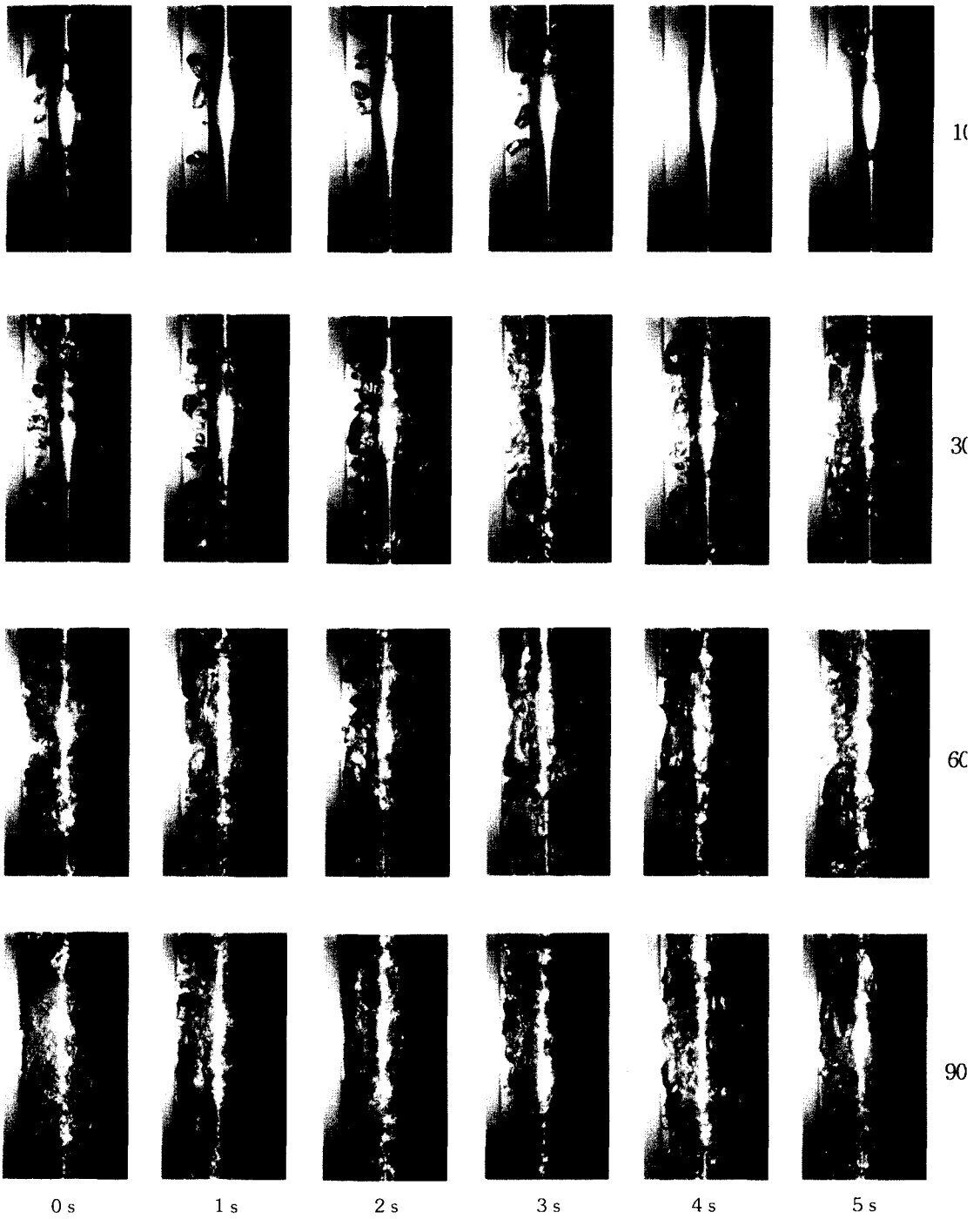


Fig. 8. Photos of Pool Boiling on Tube Surface as Heat Flux Changes( $s=15.0\text{mm}$ )

disturbed by the liquid flow for the closed bottom case. Therefore, due to the very restricted and small flow area for the bubbles, the coalesced bubble slugs cover the heated tube surface and then result in  $h_b$  deterioration around the upper as heat flux increases. Since less bubble coalescence is expected as the location of thermocouple approaches to the bottom of the tube (see Fig. 7(c)), onset of  $h_b$  deterioration is observed at somewhat higher heat fluxes. Results of the local heat transfer coefficients for  $s=3.9$  mm suggest strongly the existence of the bubble slug coalescence on the tube surface through the whole tube length. However, effects of bubble slugs are observed only around the upper region of the tube (see Fig. 7(a)) as  $s=34.9$  mm. Summarizing liquid agitation and bubble coalescence, the confined conditions result in strong liquid agitation at lower heat fluxes and bubble coalescence around the upper region of the tube at higher heat fluxes. Therefore, the bubble coalescence is the major cause of the  $h_b$  deterioration.

Several photos of the water boiling on the heated tube surface for  $s=15.0$  mm is shown in Fig 8. All photos were taken at the elevation of the T/C3. As shown in the photos, the boiling phenomena are changing periodically (i.e., few bubbles  $\leftrightarrow$  many bubbles) for the same heat flux as time elapses. The difference in bubble generation is due to the liquid agitation followed by bubble fluctuation (i.e., upward and downward). As heat flux continues to increase, bubbles become containing the whole space between the heated tube and the outer glass tube. This tendency can be suggested as the main cause of the  $h_b$  deterioration.

#### 4. Conclusions

To investigate effects of gap sizes of vertical annuli on nucleate pool boiling heat transfer of

water at atmospheric pressure several data for the five gap sizes (3.9-44.3 mm) have been obtained experimentally. Through the tests, tubes of a closed bottom have been investigated and the whole results are compared with those of a single unconfined tube. The major conclusion drawn from this experimental investigation may be stated that the annular condition gives much increase in heat transfer at moderate heat fluxes. The increase is much enhanced as the gap size decreases. At the same tube wall superheat (about 3.1 K) the heat flux of the least gap size is more than three times greater than that of the unconfined tube. However, deterioration of heat transfer occurs at high heat flux ( $q''=30$  kW/m<sup>2</sup> as  $s=3.9$  mm) for confined boiling.

#### Nomenclature

$A$	heat transfer area
$D$	tube outer diameter
$D_i$	inside diameter of the outer tube
$h_b$	boiling heat transfer coefficient
$I$	supplied current
$L$	tube length
$q$	input power
$q''$	heat flux
$s$	gap size of the annulus
$T_{sat}$	saturated water temperature
$T_w$	tube wall temperature
$V$	supplied voltage

#### Acknowledgments

This work was supported by grant No. R02-2000-00309 from the Basic Research Program of the Korea Science & Engineering Foundation.

#### References

1. M. H. Chun and M. G. Kang, "Effects of heat

- exchanger tube parameters on nucleate pool boiling heat transfer," *ASME J. Heat Transfer* 120, 468 (1998).
2. M. M. Corletti and L. E. Hochreiter, "Advanced light water reactor passive residual heat removal heat exchanger test," Proceedings of the 1st JSME/ASME Joint International Conference on Nuclear Engineering, Tokyo, Japan, 381 (1991).
  3. M. G. Kang, "Experimental investigation of tube length effect on nucleate pool boiling heat transfer," *Annals of Nuclear Energy* 25 (4-5), 295 (1998).
  4. M. G. Kang, "An experimental parametric study of heat exchanger design under pool boiling condition for application to PRHRS of AP600," Ph. D. dissertation, KAIST. (1996).
  5. K. E. Gungor and H. S. Winterton, "A general correlation for flow boiling in tubes and annuli," *Int. J. Heat Mass Transfer* 29 (3), 351 (1986).
  6. Z. Liu, and R. H. S. Winterton, "A general correlation for saturated and subcooled flow boiling in tubes and annuli, based on a nucleate pool boiling equation," *Int. J. Heat Mass Transfer* 34 (11), 2759 (1991).
  7. G. Sun and G. F. Hewitt, "Experimental studies on heat transfer in annular flow," Proceedings of the 2nd European Thermal-Sciences and 14th UIT National Heat Transfer Conference, 1345 (1996).
  8. S. C. Yao and Y. Chang, "Pool boiling heat transfer in a confined space," *Int. J. Heat Mass Transfer* 26, 841-848 (1983).
  9. Y. H. Hung and S. C. Yao, "Pool boiling heat transfer in narrow horizontal annular crevices," *ASME J. Heat Transfer* 107, 656 (1985).
  10. M. G. Kang, "Nucleate pool boiling heat transfer in vertical annuli," *Transactions of the KSME B* 25 (8), 1113 (2001).
  11. J. Bonjour and M. Lallemand, "Flow patterns during boiling in a narrow space between two vertical surfaces," *Int. J. Multiphase Flow* 24, 947 (1998).
  12. Y. Fujita, H. Ohta, S. Uchida, and K. Nishikawa, "Nucleate boiling heat transfer and critical heat flux in narrow space between rectangular spaces," *Int. J. Heat Mass Transfer* 31, 229 (1988).
  13. M. G. Kang, "Hysteresis effects in pool boiling of water," *Transactions of the KSME B* 25 (8), 1037 (2001).